Electrochemical investigation of the electron-transfer kinetics and energetics of illuminated tungsten oxide colloids

Jonathan K. Leland, and Allen J. Bard

J. Phys. Chem., **1987**, 91 (19), 5083-5087 • DOI: 10.1021/j100303a040

or a phosphate buffer), but the rate is nearly the same in the absence of iron oxide (Figure 11). Note that this reaction is not first order. The homogeneous reaction of O_2 with iodide at this pH occurs readily and is promoted by normal room light. These results differ with those reported previously,[3a] where α-Fe_2O_3 was said to oxidize iodide with large quantum yields. Our conditions were somewhat different, however. Our measurements involved a xenon light with a 300-nm-long pass filter and a longer irradiation time. Moreover, the nature of the electron acceptor in the previous study was not indicated.

Conclusions

The iron oxides show large variations in nE_F*, which are attributed to different surface properties and crystal structure. The et process in these mediation experiments occurs under kinetically controlled conditions.

A model for direct electron transfer from a particle to an electrode was derived to explain the current transients obtained and the log j_{ss} vs. potential behavior. The model demonstrates how charge collection from a particle is affected by recombination, electron transfer, hole transfer, and generation rates. The k^0 values measured for the iron oxides show a wide variation and are generally very small. They can be increased by platinization. The intensity dependence of the steady-state photocurrent suggests extensive e^-/h^+ recombination. Further evidence for this is seen in the numerical solutions for the photocurrent transients. Here, recombination must be much faster than hole transfer to attain a steady-state photocurrent.

The rates of photooxidation of oxalate and sulfite were found to vary by about 2 orders of magnitude with the different iron oxides. This appears to be due to intrinsic differences in crystal and surface structure rather than differences in surface area, hydrodynamic diameter, or band gap.

Acknowledgment. We gratefully acknowledge the support of the National Science Foundation (CHE8304666). We thank Dr. H. Hartman for the iron oxide samples, Professor W. E. Rudzinski for his advice about preparing the FeO_x/SiO_2, and J. Cook for help in setting up the photon correlation spectroscopy measurements.

Electrochemical Investigation of the Electron-Transfer Kinetics and Energetics of Illuminated Tungsten Oxide Colloids

Jonathan K. Leland and Allen J. Bard*

Department of Chemistry, University of Texas, Austin, Texas 78712 *(Received: November 24, 1986; In Final Form: May 19, 1987)*

Electrochemical charge collection techniques were used to study the effects of platinization and reduction on the electron-transfer (et) kinetics and energetics of illuminated tungsten oxide colloids. From the mediated charge collection experiments, the quasi-Fermi level for electrons, nE_F*, was found to be +0.33 V vs. NHE (pH 0) for WO_3 and shifted to +0.21 V for the reduced (H_xWO_3) and platinized (Pt/WO_3) tungsten oxides. The platinization of WO_3 also caused it to be irreversibly reduced. Silica particles coated with a monolayer of WO_3 displayed an nE_F* which was 170 mV negative of that for WO_3. The photocurrent transients for direct et to a collector electrode were potential dependent and were used to measure k^0, the standard heterogeneous rate constant for et, by using a previous treatment derived for iron oxides. The reduction of WO_3 decreased k^0, while platinization slightly increased it.

Introduction

We report here an investigation of the kinetics of direct electron transfer (et) from a WO_3 particle to an electrode in solution, using charge collection techniques.[1] Previously, a model for direct et was developed with iron oxide particles.[2] Here, we apply those concepts to WO_3 to study the effect of platinization and tungsten bronze formation on the et kinetics and compare the properties of WO_3 to those of the iron oxides.[2] Values for nE_F*, the quasi-Fermi level for electrons under illumination, were measured by mediated charge collection techniques.[1a,b] This level in particles is analogous to the flat-band potential for n-type semiconductor electrodes and is a measure of the reducing power of photogenerated electrons in semiconductor colloids and particles. A silica particle coated with a monolayer of WO_3 was prepared for study. This material should mimic a small particle semiconductor colloid with less bulk electron/hole (e^-/h^+) recombination.

As light-collection systems, semiconductor colloids offer some desirable properties.[3] Their small particle diameter affords a high surface area, which is needed for efficient electron and hole transfer to solution and surface species. The heterogeneous rate constants that characterize such reactions for semiconductors are often lower than those for noble metals,[3d] thus necessitating a large surface area to increase the overall rate. Their small diameter allows both charge carriers generated in the bulk to diffuse to the surface before recombination.[3b] This type of behavior makes each particle operate like a miniature photoelectrochemical cell.[3a]

The photoelectrochemistry of single-crystal and polycrystalline WO_3 electrodes has been studied extensively,[4] and WO_3 has also been investigated as an electrochromic material.[5] Kransnovskii

(1) (a) White, J. R.; Bard, A. J. *J. Phys. Chem.* **1985**, *89*, 1947. (b) Ward, M. D.; White, J. R.; Bard, A. J. *J. Am. Chem. Soc.* **1983**, *105*, 27. (c) Ward, M. D.; Bard, A. J. *J. Phys. Chem.* **1982**, *86*, 3599. (d) Bard, A. J.; Pruikisma, R.; White, J. R.; Dunn, W.; Ward, M. D. *Proc. Electrochem. Soc.* **1982**, *82-3*, 381.

(2) Leland, J. K.; Bard, A. J. *J. Phys. Chem.*, accompanying paper in this issue.

(3) (a) Bard, A. J. *J. Photochem.* **1979**, *10*, 59. (b) Curran, J. S.; Lamouche, D. *J. Phys. Chem.* **1983**, *87*, 5405. (c) Fendler, J. H. *J. Phys. Chem.* **1985**, *89*, 2730. (d) Hodes, G.; Grätzel, M. *Nouv. J. Chim.* **1984**, *8*, 509. (e) Bard, A. J. *J. Phys. Chem.* **1982**, *86*, 172. (f) Gerischer, H. *J. Phys. Chem.* **1984**, *88*, 6096.

(4) (a) Reichman, B.; Bard, A. J. *J. Electrochem. Soc.* **1979**, *126*, 2133. (b) Spichigar-Ulmann, M.; Augustynski, J. *J. Appl. Phys.* **1983**, *54*, 6061. (c) Di Quarto, F.; Paola, A.; Sunseri, C. *Electrochim. Acta* **1981**, *26*, 1177. (d) Gerrard, W. A. *J. Electroanal. Chem. Interfacial Electrochem.* **1978**, *86*, 421. (e) Hodes, G.; Cahen, D.; Manassen, J. *Nature (London)* **1976**, *260*, 312. (f) Gissler, W.; Memming, R. *J. Electrochem. Soc.* **1977**, *124*, 1710. (g) Butler, M. A. *J. Appl. Phys.* **1977**, *48*, 1914. (h) Butler, M. A.; Nasby, R. D.; Quinn, R. K. *Solid State Commun.* **1976**, *19*, 1011.

(5) (a) Deb, S. K. *Philos. Mag.* **1973**, *27*, 801. (b) Reichman, B.; Bard, A. J. *J. Electrochem. Soc.* **1979**, *126*, 583. (c) Nogai, J.; Kamimori, T.; Mizuhashi, M. *Rep. Res. Lab. Asahi Glass Co., Ltd.* **1983**, *33*, 99.

0022-3654/87/2091-5083$01.50/0

TABLE I: Energetic and Kinetic Data for Different Forms of Tungsten Oxide[a]

	nE_F,[b] V	d, μm	BG, eV	BE, eV	X	N_D, cm^{-3}	k^0, cm/s	α
WO_3	0.33 ± 0.01	0.32	2.7	35.0	0.00005	5×10^{17}	1.0×10^{-6}	0.83
H_xWO_3	0.21 ± 0.04	0.42		35.3	0.032	3.2×10^{20}	5.6×10^{-8}	0.75
Pt/WO_3	0.21 ± 0.02	0.54		35.5	0.008	8.0×10^{19}	2.5×10^{-6}	0.86
SiO_2/WO_3	0.16 ± 0.01	0.18	3.0					
single-crystal WO_3	0.74[c]							
thermally oxidized 0.24[d] WO_3	0.24[d]							

[a] nE_F*, quasi-Fermi level for electrons measured vs. NHE at pH 0.0; d, hydrodynamic diameter; BG, band gap by photoacoustic method; BE, binding energy of the W $4f_{7/2}$ state; X, mole fraction of W^V in tungsten oxide; N_D, corresponding doping density; k^0, standard heterogeneous rate constant; α, transfer coefficient. [b] Error limits are the least-squares standard deviation. [c] Taken from ref 4h. [d] Taken from ref 4f.

et al. described the oxidation of water by mediated particulate WO_3 in the presence of ferric ions.[6] Darwent and Mills further developed this work by studying how oxygen evolution was influenced by deposition of RuO_2, Pt, Rh, or Ru on WO_3.[7] Grätzel et al. demonstrated that irradiation of WO_3 dispersions with Ag^+ ions as electron acceptors produces oxygen more efficiently[8] and Cl_2 can be generated by oxidation of Cl^-.[9] Pulse radiolysis techniques to measure the flat-band potential of WO_3 colloids have also been reported.[10]

Experimental Section

The tungsten oxides used in this study were tungsten trioxide (WO_3), tungsten bronze (H_WO_3), platinized tungsten oxide (Pt/WO_3), and tungsten oxide deposited on silica (SiO_2/WO_3). WO_3 powder was used as obtained from Alfa Products (Danvers, MA) (99.99%). H_xWO_3 was prepared by passing H_2 over WO_3 at 375 °C for 3 h. The x value was determined by the procedure of Choain and Marion[11] by dissolving the H_xWO_3 in boiling, saturated K_2CO_3 solution followed by the addition of AgSCN. Ag metal was formed by reaction with the reduced tungsten (formally W^V). The Ag metal is filtered, washed, and dissolved in HNO_3 and the amount of Ag^+ determined by a Volhard titration.[12] From the amount of Ag^+ produced, the extent of reduction, x, is calculated. Pt/WO_3 was prepared in a modification of the procedure of Grätzel.[9] WO_3 (0.22 g) was suspended in 100 mL of deionized water containing 0.4 mL of 0.1 M H_2PtCl_6 solution. After 16 h of irradiation with a Xe lamp, 40 mL of formaldehyde was added, and the material was photolyzed for another 1.5 h. The material, which had turned blue-grey, was washed and centrifuged 5 times and vacuum dried. After platinization, the dry powder was heated in oxygen at 500 °C for several hours and then cooled under an oxygen atmosphere. The extent of platinization was determined gravimetrically by dissolving the WO_3 in boiling, saturated K_2CO_3 solution, filtering the Pt, washing it with H_2O and HNO_3, and drying. The extent of platinization was 2.5 wt %. SiO_2/WO_3 was prepared by a controlled hydrolysis technique. A WCl_6 solution in dry CH_2Cl_2 (prepared in a glove box) was allowed to hydrolyze on SiO_2 (Degussa powder; dried at 140 °C for 4 h) in dry toluene under high-purity N_2. This mixture was stirred and refluxed for 24 h. The mixture was then filtered in air, washed with toluene, acetone, and methanol, and dried. During filtration and washing, the material changed color from a dark blue to white, which represented hydrolysis of the residual W–Cl bonds. The hydrodynamic diameter of the SiO_2 was measured before and after the treatment and was found to be unchanged. The X-ray powder pattern showed no peaks for WO_3. Suspensions of these materials were prepared by sonicating the dried powders in deionized water. The concentrations were 1 mg/mL.

The hydrodynamic diamters of the colloids were measured by photon correlation spectroscopy with the equipment described previously[2] and are listed in Table I.

In binding energy of the tungsten $4f_{7/2}$ state was measured by X-ray photoelectron spectroscopy (Vacuum Generators ESCA LAB II) using Mg K_α radiation. To compensate for charging effects, WO_3 was assigned a value of 35.0 eV.[13] The Pt $4f_{7/2}$ state was observed on Pt/WO_3 at 70.9 eV. The photoacoustic measurements were performed with the same equipment as previously described.[2]

The solutions were placed in an electrochemical cell that was equipped with an optically flat Pyrex window for uniform illumination. The cell was irradiated with a 2.5-k W ozone-free Xe lamp. Immersed in the colloidal solution was a platinum flag electrode whose potential was held constant vs. a saturated calomel electrode (SCE) by a Princeton Applied Research (PAR) Model 173 potentiostat (Princeton, NJ). The Pt counter electrode was isolated by means of a glass frit. Before any measurements were made, the solution was deareated with N_2. The solutions were uniformly illuminated and stirred well. The current–time curves were recorded on a Soltec *XY* recorder (Sunnyvale, CA). The solutions were 0.5 M in tartrate or oxalate adjusted to the proper pH by HNO_3 or NaOH. The tartrate or oxalate served as the irreversible hole scavengers. $Ru(NH_3)_6Cl_3$ served as the electron mediator. The standard reduction potential $E^{\circ\prime}$ for $Ru(NH_3)_6Cl_3$ in 0.5 M oxalate is +0.045 vs. NHE as measured by cyclic voltammetry. In the mediated experiments oxalate was used because at about pH 3, tartrate becomes insoluble. The effective coulombic cell constant p was measured by using $K_3Fe(CN)_6$ as described previously.[1a] All chemicals used were of reagent grade or better.

In studies of direct electron transfer from particle to electrode, the photocurrent–time transients were recorded at different electrode potentials in the presence of scavenger but without a mediator present. A voltammogram was constructed by plotting the steady-state photocurrent vs. electrode potential. $Ru(NH_3)_6Cl_3$ was then added and the steady-state photocurrent measured at different pH's. In this case, the electrode potential was held constant at 150 mV positive of the anodic peak potential ($E_{p,a}$) for $Ru(NH_3)_6Cl_3$. The photocurrent observed is the reoxidation of the mediator which was reduced at the particle surface. Photocurrents from direct electron transfer are negligible at this potential. In the absence of tungsten oxide, no photocurrent was observed.

The generation rate of electron–hole pairs, G, was determined by using an EG&G (Salem, MA) Model 550 radiometer/photometer and an Oriel 7240 grating monochromator to measure the photon flux. The G value was calculated to be ca. 10^{19} $e^-h^+/cm^3 \cdot s$), using the known absorption coefficients of WO_3[5a] and assuming a quantum efficiency of 1.

Results and Discussion

Electron Mediation. Irradiation of tungsten oxide particles in the presence of an irreversible hole scavenger gives rise to an

(6) (a) Krasnovskii, A. A.; Brin, G. P. *Dokl. Akad. Nauk. SSSR* **1962**, *147*, 656. (b) Krasnovskii, A. A.; Fomin, G. V.; Brin, G. P.; Genkin, M. V.; Lyubimova, A. K.; Blyumenfeld, L. A. *Dokl. Akad. Nauk. SSSR* **1973**, *212*, 424.

(7) Darwent, J. R.; Mills, A. *J. Chem. Soc., Faraday Trans. 2*, **1982**, *78*, 359.

(8) Erbs, W.; Desilvestro, J.; Borgarello, E.; Grätzel, M. *J. Phys. Chem.* **1984**, *88*, 4001.

(9) Kiwi, J.; Grätzel, M. *J. Chem. Soc., Faraday Trans. 2*, **1982**, *78*, 931.

(10) Nenadović, M. T.; Rajh, T.; Nićić, O. I.; Nozik, A. J. *J. Phys. Chem.* **1984**, *88*, 5827.

(11) (a) Choain, C.; Marion, F. *Bull. Soc. Chim. Fr.* **1963**, 2121. (b) Berak, J. M.; Sienko, M. J. *J. Solid State Chem.* **1970**, *2*, 109.

(12) Skoog, D. A.; West, D. M. *Fundamentals of Analytical Chemistry*; Holt, Rinehart and Winston: New York, 1976.

(13) Ng, K. T.; Hercules, D. M. *J. Phys. Chem.* **1976**, *80*, 2094.

accumulation of electrons in the conduction band. These electrons can be collected onto an inert electrode in the solution.[1] The potential dependence of the photocurrent for this direct electron-transfer process can be used to measure the standard heterogeneous rate constant k^0,[2] as described in the next section. Addition of $Ru(NH_3)_6Cl_3$ to mediate electron transfer from particle to collector electrode causes a large enhancement in the photocurrent, because electron transfer (et) to the mediator is kinetically fast compared to direct electron transfer to an electrode. Moreover, the total surface area of the particles in contact with solution mediator is many times larger than that contacting the electrode. Following our previous treatment with iron oxide particles,[2] a plot of log $[i_{med}/(i_{med}^* - i_{med})]$ vs. pH should provide a measure of nE_F^*, the quasi-Fermi level for electrons under illumination, at any pH, when the reaction at the surface is thermodynamically controlled and where i_{med}^* is the steady-state photocurrent that would result if all of the mediator were reduced at the particle surface. At equilibrium under illumination, the difference between nE_F^* and $E^{\circ\prime}$, the formal electrochemical potential for the mediator, will dictate the final ratio of oxidized mediator C_O^{eq} to reduced mediator C_R^{eq} through the Nernst equation:

$$E^{\circ\prime} - nE_F^* = 0.0591 \log (C_R^{eq}/C_O^{eq}) \quad (1)$$

If $E^{\circ\prime}$ is pH independent and nE_F^* shifts 59 mV per unit of pH (which is common for oxide semiconductors) then a plot of log (C_R^{eq}/C_O^{eq}) vs. pH will be linear with a unit slope and an intercept on the pH axis where $E^{\circ\prime} = nF_F^*$. Once the ratio C_R^{eq}/C_O^{eq} is determined, then nE_F^* at any pH will be known. The bulk concentration of reduced mediator at any time can be related to the photocurrent by the expression for mass-transfer-controlled reaction:

$$C_R = i_{med}/FAm \quad (2)$$

where m is the mass-transfer coefficient, A is the area of the electrode, and F is Faraday's constant. C_O is evaluated from

$$C_O = C^* - C_R \quad (3)$$

where C^* is the total concentration of the mediator in both oxidation states. This can be related to the dark current for the oxidation of mediator, i_{med}^*, when the mediator is completely in the reduced form:

$$C^* = i_{med}^*/FAm \quad (4)$$

so that

$$[i_{med}/(i_{med}^* - i_{med})] = C_R/C_O \quad (5)$$

Under the conditions when the et and mass-transfer kinetics at the semiconductor particle surface are so fast that the ratio C_R/C_O represents the equilibrium ratio, a plot of logs $[i_{med}/(i_{med}^* - i_{med})]$ vs. pH can be used to determine nE_F^*. Typical plots with different forms of tungsten oxide are shown in Figure 1. The nE_F^* values at pH 0 are listed in Table I. The slopes are near the expected 1.0 for a thermodynamically controlled et to mediator as opposted to that previously observed for the iron oxide particles, which showed marked deviations in the slope, indicating a kinetically controlled et to the mediator.

Note that reduction of WO_3 to the tungsten bronze, H_xWO_3, causes nE_F^* to shift slightly to more negative potentials, as does platinization of WO_3. Both formation of the bronze and platiniztion thus appear to cause some reduction of WO_3. To examine the extent of this reduction, two appoaches were tried. The first was to measure the shift in the binding energy for the W $4f_{7/2}$ state by XPS (X-ray photoelectron spectroscopy). These values, listed in Table I, show a negligible shift in binding energy. The second technique, which is much more sensitive, is the one of Choain and Marion[11] described in the Experimental Section. This method consists of measuring the amount of W^V in the sample. These values are listed in Table I as the mole fraction of W^V in the lattice X and in terms of the corresponding doping density N_D, assuming the doping is caused by W^V. The n-type semiconducting behavior of WO_3 is attributed to oxygen vacancies in

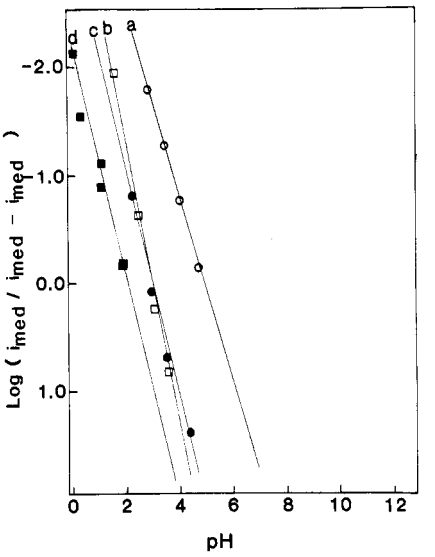

Figure 1. Plots of log $[i_{med}/(i_{med}^* - i_{med})]$ vs. pH to determine nE_F^* using $Ru(NH_3)_6Cl_3$ as mediator.

the lattice.[5a,11b] These oxygen vacancies are compensated by formation of W^V centers. Consequently, the amount of W^V in the lattice provides a reasonably good measure of the doping density, if no other impurities are present. This measurement suggests that the platinization of WO_3 results in a more reduced material (see Table I). Furthermore, the reduction process appears to be irreversible. Attempts to reoxidize by heating in an oxygen atmosphere gave no change in the extent of reduction. Since the level of reduction (or doping) is too low to cause a change in the crystalline phase,[14] the probable reason for the irreversible reduction is slow kinetics for reoxidation due to the presence of the platinum. The X-ray powder pattern for WO_3 was unchanged by the platinization. Platinization also seems to catalyze the reduction of WO_3. For example, irradiating a WO_3 suspension for 18 h gives a material with an x of 0.0002, whereas under the same conditions except by adding H_2PtCl_6 (0.4 mM) x is 0.008. $H_{0.0002}WO_3$ can be reoxidized, and $Pt/H_{0.008}WO_3$ cannot.

The photoacoustic spectrum of these materials also lends evidence about their reduced state, as shown in Figure 2. The broad band for both Pt/WO_3 and H_xWO_3 extending from about 500 nm into the IR region is a characteristic of reduced tungsten oxides.[5a,10] That nE_F^* is shifted in a negative direction by reduction has been previously demonstrated. From pulse radiolysis studies, Nenadovič et al.[10] showed that the accumulation of electrons in the conduction band shifts the flat-band potential in a negative direction. The shift is attributed to the buildup of charge from the electrons.

The nE_F^* measured for colloidal WO_3 is analogous to the flat-band potential V_{FB} of solid electrodes. The flat-band potentials for single-crystal[4h] and thermally oxidized[4f] WO_3 are also given in Table I. Our value of nE_F^* compares well with the V_{FB} for the thermally oxidized WO_3 but differs significantly with the single-crystal value. However, the V_{FB} and band gap (E_g) for WO_3 appear to depend on the nature of the material and method of preparation, as noted by Di Quarto et al.[4c] For example, reported single-crystal E_g values range between 2.2 and 2.8 eV. This variation is probably related to differences in the nature of the material. There are several possible crystal structures for WO_3, with the monoclinic form being the most stable at room temperture[14] and many stable phases containing lower valent tungsten (e.g., distorted perovskite type).[14b] The degree of crystallinity seems to be important in the physical properties, especially the measured band gap.[4c,5a] Di Quarto et al.[15] demonstrated that the

(14) (a) Gebert, E.; Ackermann, R. J. *Inorg. Chem.* **1966**, *5*, 136. (b) Magneli, A. *J. Inorg. Nucl. Chem.* **1956**, *2*, 330. (c) Berak, J. M.; Sienko, M. J. *J. Solid State Chem.* **1970**, *2*, 109.

(15) Di Quarto, F.; Di Paola, A.; Sunseri, C. *J. Electrochem. Soc.* **1980**, *127*, 1016.

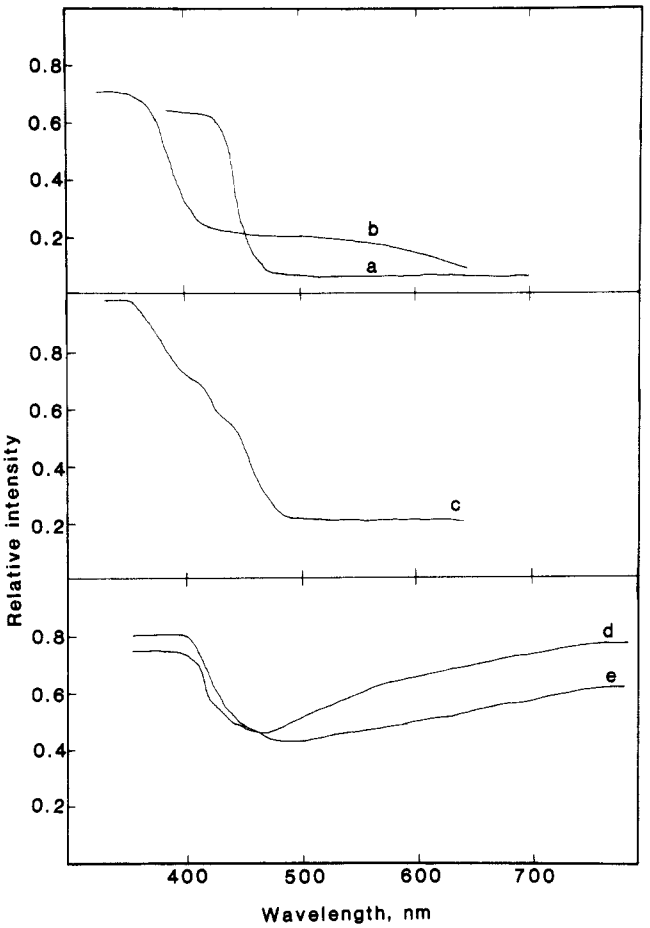

Figure 2. Photoacoustic spectrum of (a) WO_3, (b) SiO_2/WO_3, (c) $SiO_2/WO_3 \cdot 2H_2O$, (d) H_xWO_3, and (e) Pt/WO_3.

electrolyte used to prepare anodized WO_3 affected the dielectric constant. The nE_F* for SiO_2/WO_3 is 170 mV negative of that of WO_3. This shift can perhaps be ascribed to the difference in electronic properties of WO_3 as its dimensions become very small and its properties become less like the bulk material and more like those of small clusters. Such effects have been found with semiconductor particles, whose band gap changes as the particle dimensions become very small.[16-18] This localization of the energy levels in small particles would also cause the conduction band edge to be situated at higher energies or more negative potentials. Further evidence for this is seen in the photoacoustic spectrum of SiO_2/WO_3 as compared to WO_3 (Figure 2). The measured band gaps, listed in Table I, are WO_3 (2.7 eV) vs. SiO_2/WO_3 (3.0 eV).

The actual nature of WO_3 on the SiO_2 particles is not clear. Although the amount of WO_3 corresponds to about a monolayer, the WO_3 may also be in the form of small particles on the SiO_2 surface. The expected optical properties for a film thin in only one dimension and particles small in three dimensions are different. SiO_2/WO_3 is unstable in solution and slowly changes color form white to yellow after about 1 h. The dried material after immersion shows no peak in the X-ray powder pattern. If the material remains in solution for about 1 day and is then dried, the X-ray pattern shows peaks corresponding to $WO_3 \cdot 2H_2O$. The photoacoustic spectrum of this material, $SiO_2/WO_3 \cdot 2H_2O$ (Figure 2) appears to be a composite of the spectrums for WO_3 and SiO_2/WO_3.

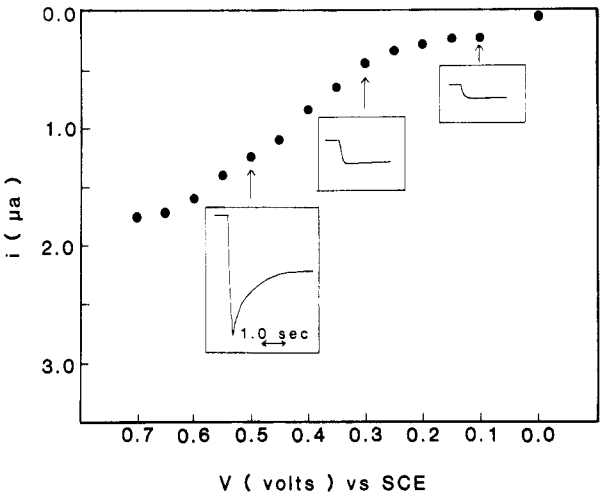

Figure 3. Steady-state photocurrents vs. electrode potential for WO_3/tartrate at pH 2.3. The insets are transients obtained at those potentials.

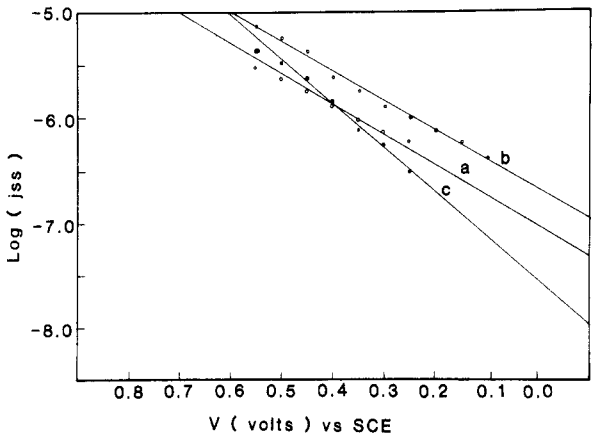

Figure 4. Tafel plots (photocurrent density vs. electrode potential) for (a) WO_3/tartrate at pH 1.1; (b) Pt/WO_3/oxalate at pH 1.0; (c) H_xWO_3/oxalate at pH 0.8.

Direct Electron Transfer. Irradiation of tungsten oxides in the presence of an irreversible hole scavenger in the absence of a mediator results in direct electron transfer from the particle to an electrode.[1c,d] The photocurrent transients obtained can be modeled by a kinetic treatment involving a second-order e^-/h^+ recombination and a Butler-Volmer model for heterogeneous et to the electrode.[2] For the tungsten oxide systems employed here, the shape of the photocurrent transient was potential dependent. In the absence of tungsten oxide, no photocurrent is observed. A plot of steady-state photocurrent (i_{ss}) vs. electrode potential for WO_3 is shown in Figure 3 along with typical photocurrent transients at the various applied potentials. This behavior was found for WO_3, Pt/WO_3, and H_xWO_3. When the electrode potential becomes very positive, the i_{ss} approaches a limiting value. The shape of the transients depends upon the potential and shows a "spike" at more positive values. A plot of log i_{ss} vs. electrode potential is shown in Figure 4 for WO_3, Pt/WO_3, and H_xWO_3. The linearity of these plots suggests that the tungsten oxides all follow Tafel-like behavior, analogous to the behavior found for the iron oxides.[2]

The change of shape of the transients with potential and the spiked appearance in the presence of a sacrificial reductant was not seen previously with the iron oxides[2] or with TiO_2,[1] although we recently saw the same behavior with TiO_2 particle dispersions at very positive potentials in the presence of tartrate. No combination of kinetic parameters in the kinetic model would simulate this behavior; niether would inclusion of electron transfer (partial cathodic currents) to oxidized intermediates produce this shape. Photocurrent transients in the absence of a hole scavenger show

(16) (a) Brus, L. E. *J. Chem. Phys.* **1983**, *79*, 5566. (b) Rossetti, R.; Nakahara, S.; Brus, L. E. *J. Chem. Phys.* **1983**, *79*, 1086.
(17) Brus, L. E. *J. Chem. Phys.* **1984**, *80*, 4403.
(18) (a) Weller, H.; Koch, V.; Gutierrez, M.; Henglein, A. *Ber. Bunsen-Ges. Phys. Chem.* **1984**, *88*, 649; (b) Nozik, A. J.; Williams, F.; Nenadovič, M. T.; Rajh, T.; Micič, O. I. *J. Phys. Chem.* **1985**, *89*, 397. (c) Fojtik, A.; Weller, H.; Koch, U.; Henglein, A. *Ber. Bunsen-Ges. Phys. Chem.* **1984**, *88*, 969. (d) Schmidt, H. M.; Weller, H. *Chem. Phys. Lett.* **1986**, *129*, 615. (e) Koch, U.; Fojtik, A.; Weller, H.; Henglein, A. *Chem. Phys. Lett.* **1985**, *122*, 507. (f) Weller, H.; Fojtik, A.; Henglein, A. *Chem. Phys. Lett.* **1985**, *117*, 485.

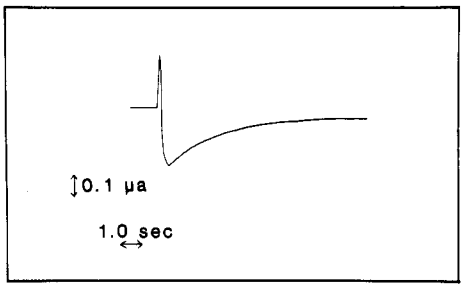

Figure 5. Photocurrent transient without hole scavenger for WO_3/0.01 M HNO_3 and 0.1 M KNO_3 at an electrode potential of 0.6 V vs. SCE.

the same spiked shape at positive potentials, in addition to a cathodic components (Figure 5). The cathodic component is the result of et to hydroxyl radicals (or other water oxidation intermediates).[1d] The fact that this cathodic spike has a small time constant suggests that the cathodic transient component is probably not responsible for the shape of the potential-dependent anodic transient. A more likely explanation is the formation of a blocking layer of particles at the surface of the electrode under illumination. In the presence of a reductant the particles build up a negative charge under illumination because of the accumulation of electrons (as holes are scavenged).[1c,1d,19] When the potential of the electrode is held sufficiently positive with respect to the point of zero charge, a layer of particles adhering to the electrode surface will form as a result of the Coulombic attraction. This layer blocks charged particles from the bulk solution from reaching the electrode surface and transferring electrons. The steady-state photocurrent then results solely from the collection of electrons from the particles on the surface of the electrode. Evidence for formation of such a layer on the electrode surface is provided by the following experiment. If the electrode is taken out of the colloidal solution after irradiation at a positive potential and placed in a clear solution containing only electrolyte and hole scavenger, a photocurrent is obtained that is similar in shape to the photocurrent transients obtained at low overpotentials. The magnitude of the steady-state photocurrent is comparable to the current obtained in the presence of semiconductor particles.

When the particles begin to adhere to the electrode surface, the voltammogram flattens and has the appearance of being under mass-transfer limiting conditions (Figure 4). However, the steady-state photocurrent in this region is still stirring rate independent. In the potential region where normal behavior is seen, the current–voltage characteristics follow the Tafel relationship.[20] The transients in this region can be fit by numerical solutions to kinetic expressions that describe the concentration of electrons and holes as a function of time.[2] Through this fit, the steady-state concentration of electrons N_{CB}^{ss}, can be calculated and is used as the concentration term in the Tafel equation:

$$\log j_{ss} = \log (nFN_{CB}^{ss}k^0) + (1 - \alpha)nf\eta/2.303 \qquad (6)$$

where j_{ss} is the steady-state photocurrent density, n is the number of electrons, k^0 is the standard heterogeneous rate constant, α is the transfer coefficient, f is F/RT, and η is the overpotential (defined as the difference between the electrode potential and nE_F^*). Through the Tafel relationship, the k^0 values were determined, which allow comparison of the et kinetics from a semiconductor particle to an electrode. Plots are shown in Figure 4, and the k^0 values are given in Table I. The differences in k^0 show that the heterogeneous et kinetics are affected by the treatments on the WO_3. As in the case of iron oxides,[2] the particle size is not as important a variable as the surface and bulk properties in this study, since k^0 varies by a factor of >200, while the particle size changes by a factor of <2. The et kinetics are primarily determined by the surface properties (either structural or electronic), as demonstrated by the increased k^0 for α-Fe_2O_3 after platinization of its surface.[2] Platinization of WO_3 slightly increases the et kinetics. However, the reductant material, H_xWO_3, has a smaller k^0 than WO_3. Thus it appears that platinization must increase the interfacial kinetics, which compensates for the slower kinetics from the reduction (since the platinization of WO_3 also causes it to be reduced).

From the slopes in Figure 4, α is calculated and is listed in Table I. The values for the transfer coefficient are significantly greater than 0.5, as was also found for the iron oxides.[2]

Conclusions

Electrochemical studies of irradiated WO_3 after different treatments in the absence and presence of a mediator provide information about the Fermi level for electrons and et kinetics. Platinization of WO_3 results in irreversible reduction and a shift in nE_F^* in a negative direction, as does direct reduction of WO_3 in an H_2 atmosphere. Monolayer WO_3 on silica displays an nE_F^* of about 170 mV negative of that for bulk WO_3 and an increase in band gap, perhaps due to quantum effects. Examination of photocurrent transients for direct et to the electrode at large overpotentials suggest that the particles stick to the electrode surface. Tafel plots can be constructed for the determination of the heterogeneous et rate constant, k^0. Reduction of WO_3 decreases k^0, while platinization increases k^0 slightly.

Acknowledgment. We gratefully acknowledge the support of the National Science Foundation (CHE8304666). We thank T. Varco-Shea for performing the XPS measurements.

(19) Dunn, W.; Aikawa, Y.; Bard, A. J. *J. Am. Chem. Soc.* **1981**, *103*, 3456.
(20) Bard, A. J.; Faulkner, L. R. *Electrochemical Methods*; Wiley: New York, 1980.

Adsorption of NO on Ni(755): Competitive Adsorption of Oxygen and Nitrogen Atoms along a Step Line of Ni(755)

H. Nozoye

Basic Research Division, National Chemical Laboratory for Industry, Higashi 1-1, Yatabe, Ibaraki 305, Japan
(Received: January 15, 1987)

The adsorption of NO on Ni(755) was studied by means of temperature-programmed desorption (TPD) and Auger electron spectroscopy (AES). A peculiar behavior of TPD spectra for N_2 can be explained by a competitive adsorption of oxygen and nitrogen atoms along a step line of Ni(755). The adsorption energy of oxygen atoms along a step line is higher than that of nitrogen atoms.

One of the main efforts in the science of catalysis is to clarify the structure of active sites. For many catalytic reactions, step sites are considered to be active sites.[1] However, there are rather few studies about chemical modifications of step sites and the

0022-3654/87/2091-5087$01.50/0